THE HELICOTREMA: MEASUREMENTS AND MODELS

D. C. MOUNTAIN AND A. E. HUBBARD

Boston University Hearing Research Center, 44 Cummington St., Boston, MA 02215, USA
E-mail: dcm@bu.edu; aeh@bu.edu

D. R. KETTEN AND J. TREHEY O'MALLEY

Dept. of Otology and Laryngology, Harvard Medical School and Massachusetts Eye & Ear Infirmary, 243 Charles Street, Boston, MA 02114, USA

Woods Hole Oceanographic Institution
Woods Hole, MA 02543, USA
E-mail: dketten@whoi.edu; jomalley2@lycos.com

The helicotrema can have a significant impact on low-frequency auditory sensitivity due to its influence on cochlear input impedance. In spite of its importance in cochlear mechanics, the helicotrema is rarely modeled accurately in current computational models of the cochlea. To address this problem, we have reconstructed the 3-dimensional anatomy of the helicotrema for several species. The anatomical results were then incorporated into hydromechanical models and the effect of these anatomical variations on cochlear input impedance was calculated.

1 Introduction

The low- and mid-frequencies regions of the mammalian audiogram are strongly influenced by the middle-ear transfer function (the ratio of intracochlear pressure near the stapes to pressure at the tympanic membrane). The behavior of this transfer function, in turn, is shaped by the interaction between the middle-ear compliance and the cochlear input impedance. The cochlear input impedance in the mid-frequency region is dominated by the inertial forces of the fluids and the compliance of the basilar membrane, while at low frequencies the helicotrema can significantly affect the cochlear input impedance [1-3].

To develop a better understanding of the role of the helicotrema, we used three-dimensional reconstructions of the cochlear fluid compartments to study the geometry of the helicotrema and its relationship to scala vestibuli (SV), scala media (SM), and scala tympani (ST). The anatomical results from our work as well as those of others were then incorporated into a hydromechanical model. The model was used to calculate cochlear input impedance and middle-ear transfer function (METF) for six species.

2 Methods

We reconstructed the 3-dimensional anatomy of the helicotrema for four species: mouse (*Mus musculus C57)*, chinchilla (*Chinchilla lanigar*), cat (*Felis catus*), and harbor porpoise (*Phocoena phocoena*). Cochleae were injected with buffered formalin, EDTA decalcified, embedded in celloidin, sectioned (20 μm), and stained with hemotoxylin-eosin. Every fifth section was acquired as a TIFF image from which the scalae were segmented interactively on screen. Cross-sectional areas of SV, SM, and ST were measured using NIH Image. Dimensions of the helicotrema were measured from 3-dimensional reconstructions calibrated by direct measurement of related structures on the original slides.

To estimate the cochlear input impedance, a classical one-dimensional [1] linear finite-difference model was used for the 4 species listed above as well as for gerbil (*Meriones unguiculatus*) and guinea pig (*Cavia porcellus*). The cochlea was divided into 512 sections and equivalent impedances were calculated for the cochlear partition and for the fluid compartments. The fluids were assumed to be incompressible and viscid, and SV and SM were combined into a single compartment. The scalae impedances were modeled as tubes with both mass and resistive terms. The resulting model was solved in the frequency domain using MATLAB. Scalae areas were taken from Plassmann *et al.* [4] for gerbil, from Thorne *et al.* [5] for mouse and guinea pig and areas for the other species were taken from our reconstructions. Basilar-membrane volume compliance for gerbil was calculated from point stiffness data [6] using a technique similar to that of Olson and Mountain [7], but with the inclusion of the effects of basilar-membrane longitudinal coupling [8] in the calculation. The predicted gerbil cochlear input impedance was qualitatively similar to published experimental data [9] but was a factor of two larger in magnitude. For cat, guinea pig, and chinchilla, the gerbil BM compliance was scaled, as necessary, to match published cochlear input impedance data. Only chinchilla required significant (times 10) scaling of the gerbil compliance values. For mouse the BM compliance was set at 0.25 times and for harbor porpoise the compliance was set equal to the gerbil values. Basilar-membrane masses were derived from the compliance map using published cochlear frequency-place maps.

The helicotrema impedance was calculated treating the helicotrema as a cylindrical tube. Middle-ear stiffness values were taken from Table 6.3 in [10]. Middle-ear mid-frequency pressure gain was assumed to be 30 dB in all species except harbor porpoise where the gain was 0 dB. Middle-ear stiffness for harbor porpoise was chosen to be 20,000 Pa/mm^3 in order to fit the experimental audiogram.

3 Results

3.1 Cochlear reconstructions

Table 1 lists the scalae areas measured at different locations for each of the four species studied. As is the case in most published data for other species, the cross sectional areas are large in the region near the oval and round windows and then taper quickly in the mid basal turn and then the area-distance function is approximately constant over the middle and lower apical regions. In most species there is an additional taper in the apex near the helicotrema [4,5].

Table 1. Scalae cross-sectional areas (mm^2)

Species	Location	Distance (%)	Scala Vestibuli	Scala Media	Scala Tympani
Mouse	Base	27.9	0.200	0.093	N.A.
	Upper base	63.6	0.066	0.059	0.156
	Middle	84.5	0.071	0.044	0.082
	Apex	98.9	0.055	0.034	0.065
Chinchilla	Lower base	23.3	0.563	0.111	0.375
	Middle base	42.8	0.410	0.097	0.338
	Upper base	56.3	0.309	0.108	0.206
	Lower middle	65.7	0.375	0.094	0.110
	Upper middle	81.0	0.110	0.103	0.110
	Apex	100	0.049	0.063	0.013
Cat	Lower base	20.2	0.733	0.132	0.828
	Middle base	33.0	0.442	0.102	0.295
	Upper base	53.3	0.333	0.109	0.238
	Lower middle	64.1	0.296	0.097	0.239
	Upper middle	80.4	0.212	0.127	0.213
	Apex	99.1	0.117	0.141	0.0024
Harbor porpoise	Base	27.9	0.627	0.150	0.974
	Middle	58.4	0.636	0.054	0.712
	Apex	87.6	0.559	0.045	0.842

Table 2. Helicotrema dimensions and cutoff frequencies

Species	Helicotrema Diameter	Minimum Height	Maximum Height	Cutoff Frequency
Mouse	0.15 mm	0.03 mm	0.08 mm	340 Hz
Chinchilla	0.48	0.26	0.31	33
Cat	0.59	0.11	0.45	22
Harbor porpoise	0.78	0.15	0.38	13

Figure 1 illustrates perilymphatic compartments near the apex for each of the reconstructed cochleae. The general form of the helicotrema is that of a flared tube with an elliptical cross section. The height of the helicotrema decreases from the abneural to the neural edge. The helicotrema dimensions are given in Table 2. The cutoff frequency in the table refers to the frequency above which the fluid mass dominates the helicotrema impedance [2].

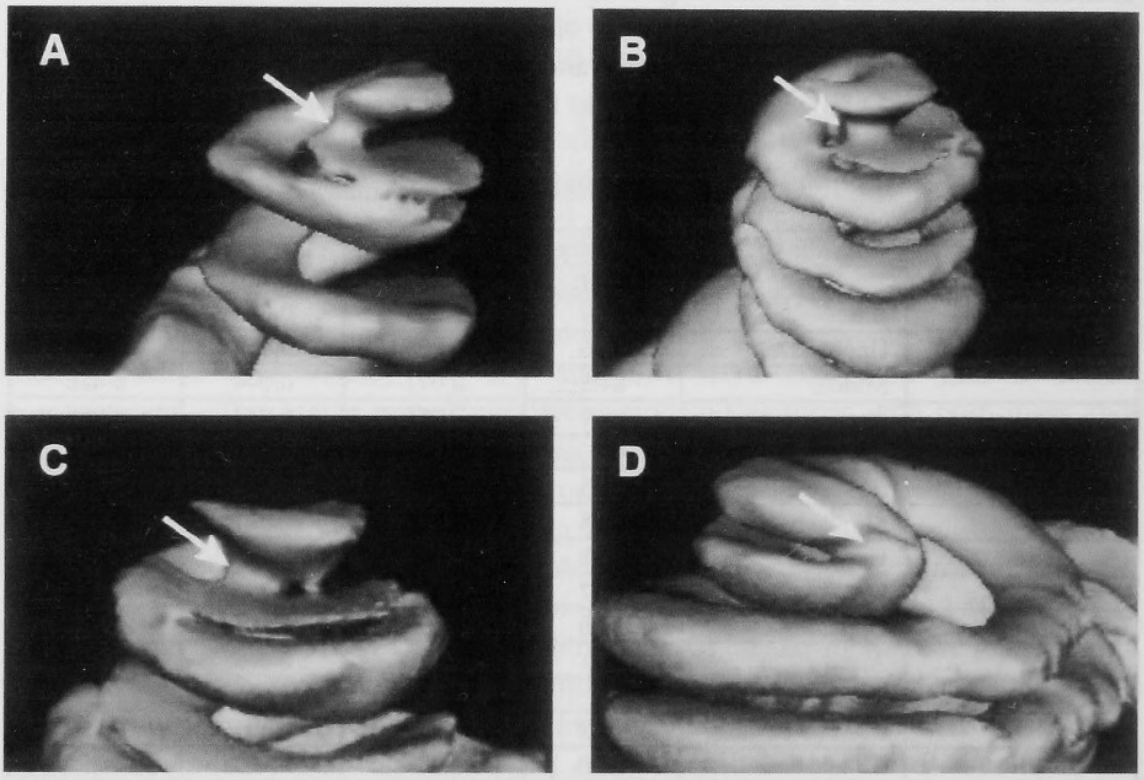

Figure 1. Apical views of the perilymphatic compartment reconstructions for four species: A: mouse, B: chinchilla, C: cat, and D: harbor porpoise. White arrows indicate the location of the helicotrema.

3.2 Simulation results

For the smaller cochleae (mouse, gerbil, guinea pig), the helicotrema had little effect on the cochlear input impedance due to the large series resistance of the scalae. The helicotrema had a significant effect on the cochlear input impedance in cat and harbor porpoise and a moderate effect on the input impedance in chinchilla.

The model METFs for all six species are shown in Figure 2 (diamond symbols). The predicted corner frequencies are similar to those found in the experimental audiograms but the low-frequency METF slope was consistently less

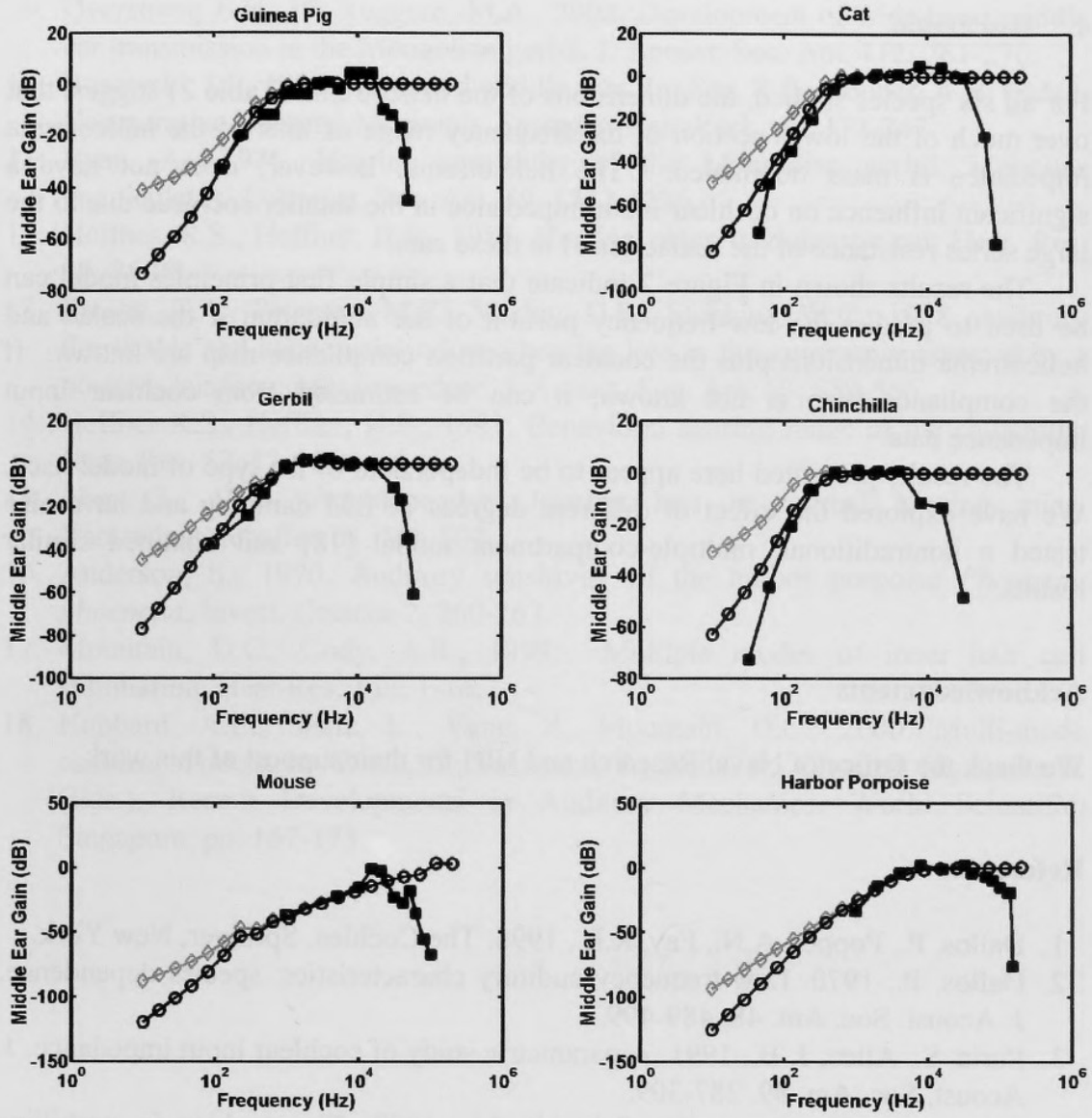

Figure 2. Model predictions for the METF (grey diamonds) and METF plus IHC filter (circles) compared to experimental audiograms (squares). Model predictions are normalized to 0 dB and audiograms have been inverted and shifted vertically for comparison purposes. Audiogram sources: gerbil [11], cat [12], guinea pig [13], chinchilla [14], mouse [15], harbor porpoise [16].

than that observed in the audiograms. This difference was most prominent for frequencies below a few hundred Hertz which leads us to speculate that the difference might be due to the high-pass filtering that is believed to take place in the coupling between BM displacement and inner hair cell hair (IHC) bundle displacement (c.f. [17]). When we cascaded a first-order high-pass filter (cutoff frequency = 400 Hz) with the METF to mimic the BM-IHC coupling, we improved the match between model and experimental data (Figure 2, circular symbols).

4 Discussion

For all six species studied, the dimensions of the helicotrema (Table 2) suggest that over much of the lower portion of the frequency range of interest the helicotrema impedance is mass dominated. The helicotrema, however, does not have a significant influence on cochlear input impedance in the smaller cochleae due to the large series resistance of the scalae found in these ears.

The results shown in Figure 2 indicate that a simple first-principles model can be used to predict the low-frequency portion of the audiogram if the scalae and helicotrema dimensions plus the cochlear partition compliance map are known. If the compliance map is not known, it can be estimated from cochlear input impedance data.

The results presented here appear to be independent of the type of model used. We have explored the effect of different degrees of BM damping and have also tested a nontraditional, multiple-compartment model [18] and obtained similar results.

Acknowledgments

We thank the Office of Naval Research and NIH for their support of this work.

References

1. Dallos, P., Popper, A.N., Fay, R.R., 1996. The Cochlea. Springer, New York.
2. Dallos, P., 1970. Low-frequency auditory characteristics: species dependence. J. Acoust. Soc. Am. 48, 489-499.
3. Puria, S., Allen, J. B., 1991. A parametric study of cochlear input impedance. J. Acoust. Soc. Am. 89, 287-309.
4. Plassmann, W., Peetz, W., Schmidt, M., 1987. The cochlea in gerbilline rodents. Brain Behav. Evol. 30, 82-101.
5. Thorne, M., Salt, A.N., DeMott, J.E., Henson, M.M., Henson, O.W., Gewalt, S.L., 1999. Cochlear fluid space dimensions for six species derived from reconstructions of 3-D magnetic resonance images. Laryngoscope 109, 1661-1668.
6. Naidu, R.C., Mountain, D.C., 1998. Measurements of the stiffness map challenge a basic tenet of cochlear theories. Hear. Res. 124, 124-131.
7. Olson, E.S., Mountain, D.C., 1991. In vivo measurement of basilar membrane stiffness. J. Acoust. Soc. Am. 89, 1262-1275.
8. Naidu, R.C., Mountain, D.C., 2001. Longitudinal coupling in the basilar membrane. J. Assoc. Res. Otolaryngol. 2, 257-267.

9. Overstreet, E.H. 3rd, Ruggero, M.A., 2002. Development of wide-band middle ear transmission in the Mongolian gerbil. J. Acoust. Soc. Am. 111, 261-270.
10. Rosowski, J.J., 1994. Outer and middle ears. In: Fay, R.R., Popper, A.N. (Eds.), Comparative Hearing: Mammals. Springer, New York, pp. 172-247.
11. Ryan, A., 1976. Hearing sensitivity of the Mongolian gerbil, Meriones unguiculatus. J. Acoust. Soc. Am. 59, 1222-1226.
12. Heffner, R.S., Heffner, H.E., 1985. Hearing range of domestic cat. Hear. Res. 19, 85-88.
13. Prosen, C.A., Petersen, M.R., Moddy, D.B., Stebbins, W.C., 1978. Auditory thresholds and kanamycin-induced hearing loss in the guinea pig assessed by a positive reinforcement procedure. J. Acoust. Soc. Am. 63, 559-566.
14. Heffner R.S., Heffner, H.E., 1991. Behavioral hearing range of the chinchilla. Hear. Res. 52, 13-16.
15. Ehret, G., 1974. Age-dependent hearing loss in normal hearing mice. Naturwissenschaften 61, 506-507.
16. Anderson, S., 1970. Auditory sensitivity of the harbor porpoise *Phocoena phocoena*. Invest. Cetacea 2, 260-263.
17. Mountain, D.C., Cody, A.R., 1999. Multiple modes of inner hair cell stimulation. Hear Res. 132, 1-14.
18. Hubbard, A.E., Shatz, L., Yang, Z., Mountain, D.C., 2000. Multi-mode cochlear models. In: Wada, H., Takasaka, T., Ikeda, K., Ohyama, K., Koike T. (Eds.), Recent Developments in Auditory Mechanics. World Scientific, Singapore, pp. 167-173.